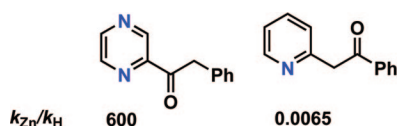# Binding Catalysis and Inhibition by Metal Ions and Protons in the Enolization of Phenylacetylpyrazine

Anne-Gaelle Collot, Michael Courtney, Dara Coyne, Stephen E. Eustace, and Rory A. More O'Ferrall*

School of Chemistry and Chemical Biology, University College Dublin, Belfield, Dublin 4, Ireland

rmof@ucd.ie

Received December 2, 2008

A study of the enolization of phenylacetylpyrazine (PzCOCH$_2$Ph) catalyzed by acid, base and metal ions in aqueous solution shows, unusually, that metal ions are more effective catalysts than protons, e.g., for zinc $k_{Zn}/k_H = 600$. Such behavior contrasts with that of the structurally related phenacylpyridine (PyCH$_2$COPh) for which $k_{Zn}/k_H = 0.0065$. To interpret this difference, equilibrium constants for the tautomerization of phenylacetylpyrazine and for binding of protons and metal ions to its keto tautomer and enolate anion have been measured or estimated and are compared with existing measurements for phenacylpyridine. A tautomeric constant, $K_E = 1.2 \times 10^{-3}$ (p$K_E = 2.9$), is derived by combining forward and reverse rate constants for enolization measured, respectively, by iodination or bromination of the keto tautomer and relaxation of the less stable enol. For the keto tautomer, NMR measurements yield a p$K_a = -0.90$ for N-protonation, and spectrophotometric measurements give p$K_a = 11.90$ for ionization to an enolate anion. For the enol, pK_a values of 0.44 and -4.80 for mono- and diprotonation are obtained from the pH profile for ketonization and absorbance measurements for the transient enol reactant. Binding constants for metal ions (Cu^{2+}, Ni^{2+}, Zn^{2+}, Co^{2+}, and Cd^{2+}) are derived from the saturation of their catalysis of the ketonization reaction. It is found that ketonization is efficiently catalyzed by metal ions but inhibited by acid. These findings, and the striking difference from phenacylpyridine, are ascribed to differences in thermodynamic driving force arising from stronger binding of the proton to the more basic pyridine than pyrazine nitrogen atom in both the reactant keto tautomer and in the enaminone or zwitterion product of the rate-determining (proton transfer) step of the enolization.

Introduction

Studies of the ionization and tautomerism of α- and β-heterocyclic ketones[1−9] form part of a wider investigation of keto-enol[10] or keto-phenol[11] tautomerism of aldehydes, ketones,[12] ketenes,[13] and carboxylic acids[14,15] as well as

carboxylic acid esters,[16,17] amides,[17] and anions,[14] undertaken by a number of authors over the past 20 years. The present paper describes measurements of equilibrium constants for

* To whom correspondence should be addressed. Tel: 353-1-716-2285/2165.

(1) Katritzky, A. R.; Kucharska, H. Z.; Rowe, J. D. *J. Chem. Soc.* **1965**, 3093–3096. Elguero, J.; Marzin, C.; Katritzky, A. R.; Linda, P. *Advances in Heterocyclic Chemistry, Supplement 1*; Academic Press: London, 1976.

(2) Carey, A. R. E.; Eustace, S. E.; More O'Ferrall, R. A.; Murray, B. A. *J. Chem. Soc., Perkin Trans. 2* **1993**, 2285–2296.

(3) Carey, A. R. E.; Fukata, G.; More O'Ferrall, R. A.; Murphy, M. G. *J. Chem. Soc., Perkin Trans. 2* **1985**, 1171–1722.

(4) Carey, A. R. E.; More O'Ferrall, R. A.; Murphy, M. G.; Murray, B. A. *J. Chem. Soc., Perkin Trans. 2* **1994**, 2471–2479.

(5) McCann, G. M.; More O'Ferrall, R. A.; Walsh, S. M. *J. Chem. Soc., Perkin Trans. 2* **1997**, 2761–2772.

(6) Eustace, S. E.; McCann, G. M.; More O'Ferrall, R. A.; Murphy, M. G.; Murray, B. A.; Walsh, S. M. *J. Phys. Org. Chem.* **1998**, *11*, 519–528.

(7) Bunting, J. W.; Stefanidis, D. *J. Am. Chem. Soc.* **1988**, *110*, 4008–4017.

(8) Stefanidis, D.; Bunting, J. W. *J. Am. Chem. Soc.* **1990**, *12*, 3163–3168.

(9) More O'Ferrall, R. A.; Murray, B. A. *J. Chem. Soc., Perkin Trans. 2* **1994**, 2461–2470. Katritzky, A. R.; Ghiviriga, J.; Oniciu, D. C.; More O'Ferrall, R. A.; Walsh, S. M. *J. Chem. Soc., Perkin Trans. 2* **1997**, 2605–2608. Greenhill, J. V.; Loghmani-Khouzani, H.; Maitland, D. J. *J. Chem. Soc., Perkin Trans. 2* **1991**, 2831–2840.

(10) *The Chemistry of Enols*; Rappoport, Z., Ed.; Wiley: New York, 1990.

(11) Capponi, N.; Gut, I. G.; Hellrung, B.; Persy, G.; Wirz, J. *Can. J. Chem.* **1999**, *77*, 605–613.

(12) Chiang, Y.; Kresge, A. J.; Nikolau, V. A.; Popik, V. V. *J. Am. Chem. Soc.* **2003**, *125*, 6478–6484.

(13) Kresge, A. J. *Acc. Chem. Res.* **1990**, *23*, 43–48.

(14) Richard, J. P.; Williams, G.; O'Donoghue, A. C.; Amyes, T. L. *J. Am. Chem. Soc.* **2004**, *124*, 2957–2968.

the ionization and tautomerization of phenylacetylpyrazine **1**. It compares catalysis of enolization by protons and metal ions and explores the concept of "binding at the transition state" as a basis for interpreting the relative effectiveness of the two catalysts.

A feature distinguishing heterocyclic ketones from simpler ketones is that migration of hydrogen from carbon to nitrogen to form an imine provides an alternative to enolization as a pathway for tautomerization. Indeed, for the β-heterocyclic ketones 2- and 4-phenacyl-pyridine[2] or quinoline[3] (e.g., **2**) in aqueous solution, the enaminone **3** rather than the enol **4** is the principal minor tautomer.
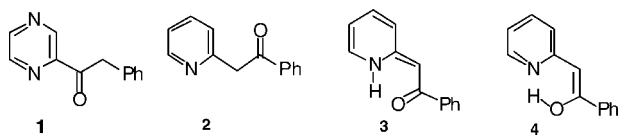

The enol is restored as the preferred second tautomer[4] if the basicity of the heterocyclic nitrogen atom is reduced, as in phenacylprazine **5**. The same is true of α-heterocyclic ketones, such as the phenylacetylpyridines (e.g. **6**), for which the alternative tautomer is a zwitterion **7** lacking the stabilizing resonance interaction between positive and negative charge
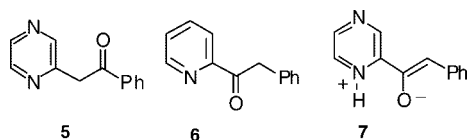

centers which leads to charge neutralization in the enaminones.[5]

A characteristic of heterocyclic ketones is that even when the zwitterion or enaminone is present at lower concentrations than the enol, these species are implicated as intermediates in the acid-catalyzed interconversion of keto and enol tautomers. This is illustrated in eq 1, in which acid-catalyzed reaction of the ketone proceeds not with initial protonation of the keto oxygen atom but protonation of the nitrogen atom of the heterocyclic ring. This protonation is followed by proton removal from carbon to yield the enaminone (or zwitterion) as intial product, which then tautomerizes rapidly to the more stable enol. The reaction may be monitored by trapping the enol or enaminone with iodine or bromine or may be observed directly in the thermodynamically favored reverse direction following quenching of the enolate anion in excess acid or acidic buffers.[4,5]
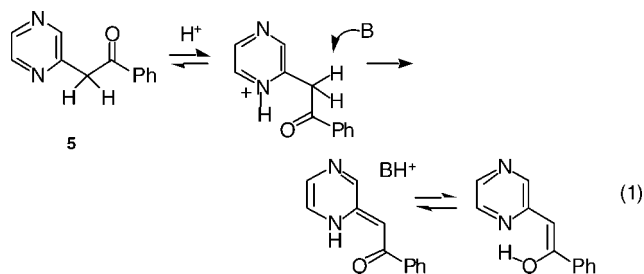
For phenylacetylpyrazine **1** the enol **8** is again the more stable minor tautomer. Indeed, in this case the zwitterion is so unstable that it is doubtful if it is formed as an intermediate in the acid-catalyzed enolization. Moreover, the catalytic effectiveness of protonation on nitrogen is so attenuated that in the ketonization direction protonation inhibits rather than catalyzes the reaction.
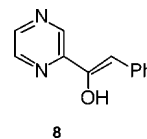
This ineffective acid catalysis is complemented by pronounced catalysis by metal ions. The ratio of rate constants for catalysis by zinc ions and protons, $k_{Zn}/k_H = 591$, appears to be the highest recorded for Lewis acid catalysis in aqueous solution.[6,18] This marked advantage for metals contrasts with the previously reported behavior[6] of 2-phenacylpyridine **1**, for which protons are favored over zinc ions by a factor of 1600, a difference in relative rates between the two substrates of nearly 10^6. A principal aim of the present paper is to establish the extent to which this difference can be accounted for in terms of binding constants of catalysts to their respective substrates and the thermodynamic driving force conferred by complexation of the catalysts to these substrates

Results

Equilibrium Measurements. In aqueous solution phenylacetylpyrazine exists predominantly as its keto tautomer (**1**), as indicated by its UV−vis spectrum (with $\lambda_{max} = 270$, $\varepsilon = 1.9 \times 10^4$) and proton and ^{13}C NMR spectra. In dilute aqueous sodium hydroxide it forms a long wavelength species with $\lambda_{max} = 320$ nm ($\varepsilon = 1.15 \times 10^4$) and a shoulder at 395 nm ($\varepsilon = 6.6 \times 10^3$) for which the dependence of the intensity on base concentration is consistent with ionization to an enolate anion with $pK_a = 11.90$. (Errors for ionization or rate constants are given in the Experimental Section or Supporting Information.)

There is no change in wavelength or intensity of the principal absorption maximum upon addition of acid to a neutral solution of phenylacetylpyrazine, and in this respect the behavior is similar to that of 2-phenylacetylpyridine, for which practically no change in absorption spectrum accompanies protonation of the ring nitrogen atom.[5] Qualitative evidence for the protonation was obtained from the acid dependence of the fluorescence spectrum, but a quantitative value for the pK_a was obtained by NMR from the dependence of chemical shifts of hydrogen atoms of the pyrazine ring in DCl solutions upon acid concentration, based on the measurements listed in Table S1 of the Supporting Information. These measurements gave $pK_a = -0.42$. Similar measurements for 2-acetylpyrazine (Table S2, Supporting Information) gave $pK_a = -0.55$. The values are based on best fits of calculated to observed chemical shifts plotted against pH $- X_o$[19,20] for phenylacetyl-pyrazine in Figure 1 and for acetylpyrazine in Figure S1 (Supporting Information). The measured values refer to D_2O, and for phenylacetylpyrazine the pK_a was corrected to -0.90 in H_2O by assuming that the isotope

(15) Andraos, J.; Chiang, Y.; Kresge, A. J.; Popik, V. V. *J. Am. Chem. Soc.* **1997**, *119*, 8417–8424.

(16) Richard, J. P.; Amyes, T. L. *J. Am. Chem. Soc.* **1996**, *118*, 3129–3141. Chiang, Y.; Jones, J. Jr.; Kresge, A. J. *J. Am. Chem. Soc.* **1994**, *116*, 8358–8359.

(17) Chiang, Y.; Guo, H.-X.; Kresge, A. J.; Richard, J. P.; Toth, K. *J. Am. Chem. Soc.* **2003**, *125*, 187–194.

(18) Fontana, A.; De Maria, P.; Pierini, M.; Siani, G.; Cerritelli, S.; Macaluso, G. *J. Phys. Org. Chem.* **2002**, *15*, 247–257.

(19) Cox, R. A. *Adv. Phys. Org. Chem.* **2000**, *35*, 1–66. Bagno, A.; Scorrano, G.; More O'Ferrall, R. A. *Rev. Chem. Intermed.* **1987**, *7*, 313–352.

(20) Cox, R. A.; Lam, S.-O.; McClelland, R. A.; Tidwell, T. T. *J. Chem. Soc., Perkin Trans. 2* **1979**, 272–275.

(21) Kresge, A. J.; More O'Ferrall R. A.; Powell, M., *Isotopes in Organic Chemistry Vol 7; Secondary and Solvent Isotope Effects*; Buncel, E., Lee, C. C., Eds.; Elsevier: Amsterdam, 1987; pp 177−273.
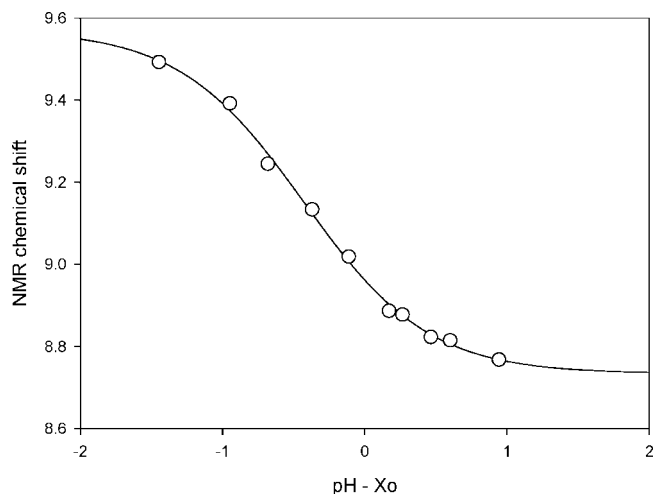
FIGURE 1. Plot of chemical shift against $pH - X_o$ for the protonation of phenylacetylpyrazine in $DCl-D_2O$ at 25 °C.
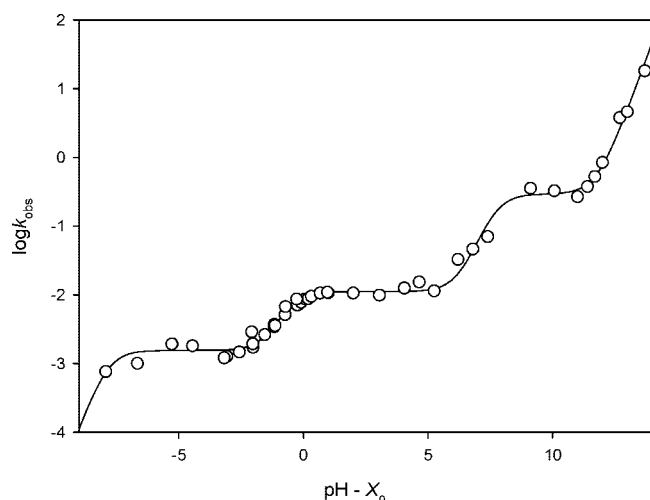
FIGURE 2. Plot of $\log k_{obs}$ against $pH - X_o$ for the ketonization of phenylacetylpyrazine enol in $HClO_4$, NaOH, and aqueous buffers at 25 °C.

TABLE 1. Rate Constants for Buffer-Independent and Buffer (Base)-Catalyzed Ketonization of Phenylacetylpyrazine Enol in Aqueous Buffers (Ionic Strength 0.1) at 25 °C

buffer base	buffer ratio ([B]/[BH$^+$])	pH	k_o	k_{GB}
acetate	0.25	4.05	0.012	1.90
	1.0	4.65	0.019	1.85
	4.0	5.25	0.011	1.99
lutidine	0.25	6.20		22.6
	1.0	6.80		22.6
	4.0	7.40		26.9
borate	1.0	9.12	0.36	3.5[a]
	9.0	10.07	0.33	1.4[a]

[a] Subject to large uncertainties: 3.5 ± 2.9 or 1.4 ± 0.8.

effect on the equilibrium was the similar to that measured for N-protonation of the enol tautomer (3.8) and the normal value of $K_a^{H2O}/K_a^{D2O} = 3.0$ for dissociation of weak acids.[21]

Acid–Base Catalysis of Ketonization. Rate constants for relaxation of the enol of phenylacetylpyrazine to its more stable keto tautomer were measured in aqueous solution at 25 °C by quenching a solution of the enolate anion in 0.1 M sodium hydroxide in excess acid or acidic buffer. The reaction was susceptible to catalysis by hydroxide ion, hydrogen ion and the

base component of the buffer; it also showed an uncatalyzed reaction. In buffer solutions and more basic media rate constants were measured using a Durrum stopped-flow spectrometer, but in solutions of hydrochloric or perchloric acid, below pH 3, the reaction was slow enough for measurements using a conventional spectrophotometer. In the pH range 1–9 the reaction was monitored from disappearance of a spectrum with $\lambda_{max} = 335$ nm ($\varepsilon = 2.14 \times 10^4$) which was attributed to the enol. Above 0.1 M H$^+$, the initial spectrum from quenching the enolate anion changed to one with $\lambda_{max} = 390$ nm ($\varepsilon = 1.9 \times 10^4$). The dependence of the intensity of this chromophore upon acid concentration, and the observation of an inflection in the pH dependence of rate constants in the same acid concentration range, suggested that it corresponded to the protonated enol. At very high acid concentrations (>10 M HClO$_4$) a further change to a spectrum with $\lambda_{max} = 510$ nm was attributed to formation of the diprotonated enol. The high value of λ_{max} for this ion is consistent with values observed by Bunting for N-methylarylacetylpyridimium ions in basic solution.[7]

First-order rate constants (k_{obs}) for ketonization were measured in acetate, lutidine and borate buffers. The values are shown in Tables S3–S5 of the Supporting Information. Plots of k_{obs} against concentration of buffer base (B) gave straight lines of slope k_{GB}^K and intercept k_o consistent with eq 2. There was no dependence on buffer acid concentration. This is consistent with the operation of general base but not general acid catalysis. Values of k_o and k_{GB} are listed in Table 1.

$$k_{obs} = k_o + k_{GB}^K[B] \tag{2}$$

Rate constants for ketonization in perchloric acid are shown in Table S6 (Supporting Information). Rate constants for "ketonization" correspond to a sum of rate constants for conversion of the enol (or enolate anion) to ketone and the reverse enolization. However, only at pH values greater than the pK_a of the enol (9.0) does the "reverse" reaction contribute appreciably to the measured rate constant.

pH Profile for Ketonization. The rate constants in Table S6 (Supporting Information) may be combined with the buffer-independent values (k_o) in Table 1 and rate constants for conversion of phenylacetylpyrazine to its enolate anion in dilute sodium hydroxide, listed in the Experimental Section, to provide a plot of $\log k$ against pH shown as a pH profile in Figure 2. The profile corresponds to rate constants for relaxation of the enol tautomer EH (and its conjugate acids EH$_2^+$ and EH$_3^{2+}$) to the keto tautomer (KH) and, in basic solutions, to ionization of the keto tautomer to its enolate anion (E$^-$). At high acid concentrations the pH is replaced by $pH - X_o$, which corresponds to the Hammett acidity function H_o.[19,22]

Figure 2 presents a staircase-like profile, with three pH-independent segments separating three, or possibly four, base-catalyzed or acid-inhibited reactions. Despite its apparent complexity an interpretation is straightforward. Between pH 9 and pH 13 the observed reactions are ionization of phenyl-acetylpyrazine to its enolate anion and the reverse protonation of the anion by water with rate constants k_{OH} (40.5 M^{-1} s^{-1}) and k_{H2O} (0.33 s^{-1}). Below pH 9 the enol exists predominantly in its un-ionized form and the reaction again becomes base-dependent reflecting ionization of the enol prior to its reaction
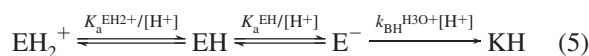
(22) More O'Ferrall, R. A.; O'Brien, D. M. *Can. J. Chem.* **2000**, *78*, 1594–1612.

with water. These reactions are summarized in eqs 3 and 4, in which K_a^{EH} is the ionization constant of the enol and KH, EH and E$^-$ denote the ketone, enol and enolate anion, respectively.

$$EH \underset{k_{OH}[HO^-]}{\overset{K_a^{EH}/[H^+]}{\rightleftharpoons}} E^- \overset{k_{H2O}}{\rightleftharpoons} KH \qquad (3)$$
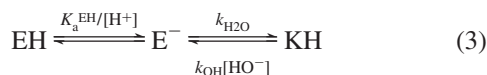
$$k_{obs} = \frac{k_{H2O}}{(1 + [H^+]/K_a^{EH})} + k_{OH}[HO^-] \qquad (4)$$

Below pH 7, reaction of the enolate anion with H_3O^+ (with rate constant k_H) becomes more important than with H_2O, and this accounts for the pH-independent reaction ($k = 1.19 \times 10^{-2}$ s^{-1}) between pH 7 and pH 1. Between pH 1 and 0 a further change to a pH-dependent reaction ($k = 1.51 \times 10^{-3}$ s^{-1}) is interpreted as a change in reactant from enol to protonated enol (EH_2^+). This interpretation is supported by a complementary change in spectrum and λ_{max} of the reactant (from 335 to 395 nm) and a dependence of the relative intensities of the two chromophores upon acid concentration consistent with an ionization equilibrium with $pK_a = 0.45 \pm 0.1$ (Table S7 of the Supporting Information). These reactions are summarized in eqs 5 and 6, in which the acid dissociation constant of the protonated enol (**9**) is denoted K_a^{EH2+} and the rate constant for reaction of H_3O^+ with the enolate anion is k_{BH}^{H3O+} (the notation for this rate constant is explained below).

$$EH_2^+ \overset{K_a^{EH2+}/[H^+]}{\rightleftharpoons} EH \overset{K_a^{EH}/[H^+]}{\rightleftharpoons} E^- \overset{k_{BH}^{H3O+}[H^+]}{\longrightarrow} KH \quad (5)$$

$$k_{obs} = \frac{k_{BH}^{H3O+}[H^+]}{(1 + [H^+]/K_a^{EH2+})[H^+]/K_a^{EH}} \qquad (6)$$
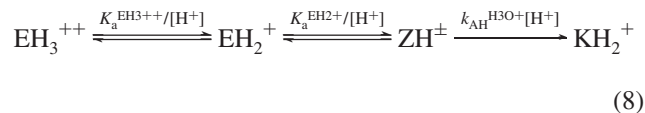
In more concentrated solutions of perchloric acid, above 4 M, a further acid-independent reaction is seen. This is interpreted as a shift in mechanism from reaction of H_3O^+ with enolate anion as in eq 5 to reaction with the unprotonated enol or, alternatively,[5] as shown in eq 8, the zwitterionic species **10**. Which pathway is preferred is considered below.

(7)
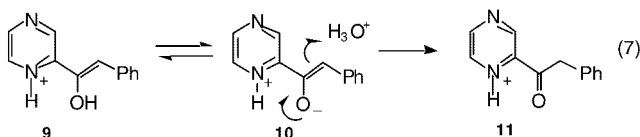
Finally, at high acidities (>10 M HClO$_4$) there is evidence of a further change in chromophore of the reactant (derived from quenching the enolate anion from base) from $\lambda_{max} = 395$ nm to $\lambda_{max} = 510$ nm. This is interpreted as reflecting an additional protonation of the enol, at the second nitrogen of the pyrazine ring, to yield the diprotonated species EH_3^{+2}. From the dependence on acidity of the absorbance at 510nm, as measured by Cox's and Yates's acidity parameter X_o,[19,22] a $pK_a = -4.80 \pm 0.15$ may be inferred based on the data in Table S8 (Supporting Information) and a plot of absorbance at 510 nm against pH $-$ X_o in Figure S2 (Supporting Information).

In principle, the reactions and the kinetic expression for the dependence of k_{obs} upon acid concentration over the high acidity range are described by eqs 8 and 9. In eq 8, ZH$^\pm$ refers to the zwitterionic species **10** and KH$_2^+$ to the monoprotonated ketone **11**. In eq 9 K_a^{EH3++} is the acid dissociation constant of the

diprotonated enol, K_a^{EH2+} is the acid dissociation constant of the monoprotonated enol and k_{AH}^{H3O+} refers to the rate constant for protonation of the zwitterion (at carbon) by H_3O^+ to form the *N*-protonated ketone **11** (or of the enol to form the *O*-protonated ketone). The derived equation is simplified by the fact that this mechanism is observed only under conditions that the enol (EH) is fully protonated.

$$EH_3^{++} \overset{K_a^{EH3++}/[H^+]}{\rightleftharpoons} EH_2^+ \overset{K_a^{EH2+}/[H^+]}{\rightleftharpoons} ZH^\pm \overset{k_{AH}^{H3O+}[H^+]}{\longrightarrow} KH_2^+$$

(8)

$$k_{obs} = \frac{k_{AH}^{H3O+}K_a^{EH2+}}{(1 + [H^+]/K_a^{EH3++})} \qquad (9)$$

In practice, this kinetic expression needs to be modified to take account of the more complex dependence of rate and equilibrium constants upon acid concentration characteristic of strong acid solutions. As discussed in more detail below, this is done by replacing pH by pH $-$ X_o (and [H$^+$] by $10^{-(pH-Xo)}$). The parameter X_o is a measure of the capacity of the medium to protonate a series of reference aniline bases and corresponds to log (K_a/K_a^{H2O}) where K_a is the measured acid dissociation constant of a protonated aniline at a particular acid concentration and K_a^{H2O} is the dissociation constant in water.[19] In so far as X_o approaches zero in dilute acid solutions, pH $-$ X_o reduces to pH at values greater than 1.

The line drawn through the experimental points in Figure 2 represents a best fit to the measured rate constants based on assignment of rate and equilibrium constants to the sum of the right-hand sides of eqs 4, 6, and 9. As discussed in the Experimental Section, the derived equilibrium constants are consistently somewhat larger than those determined spectrophotometrically. At least in the case of monoprotonation of the enol the difference ($pK_a = -0.58$ compared with 0.45) appears to beyond the range of experimental error. The explanation for this discrepancy is considered below but remains uncertain.

Solvent Isotope Effects and Catalysis in HCl and DCl. In addition to kinetic measurements of ketonization in HClO$_4$ measurements were undertaken in aqueous HCl. This was to assess solvent isotope effects on rate and equilibrium constants by comparison with DCl (in D$_2$O). To our surprise, instead of first-order rate constants remaining constant or decreasing as the acid concentration increased, above a value of 5 M they showed a sharp increase. The same behavior was observed in DCl$-$D$_2$O. Figure 3 shows plots of log k_{obs} against pH $-$ X_o (pH profiles) in the strong acid region for HCl and DCl. Measured rate constants for these acids are shown in Table S9 (Supporting Information).

The discrepancy between rate constants in HCl and HClO$_4$ at the same X_o value suggests catalysis by chloride ions. When the reaction was carried out in HBr a similar increase in rate was observed. From a comparison of UV$-$vis spectra the products in HClO$_4$ and HCl appear to be the same, i.e., the *N*-protonated ketone. It remains difficult to envisage the involvement of chloride ion as a base or through an unusual salt effect.

At lower acid concentrations, rate constants in HCl and HClO$_4$ at the same pH $-$ X_o value are similar. The measurements in DCl lead to a pH-independent rate constant 1.53×10^{-3} s^{-1} and corresponding solvent isotope effect $k_{H2O}/k_{D2O} = 7.0$, which is consistent with rate-determining proton transfer from H_3O^+
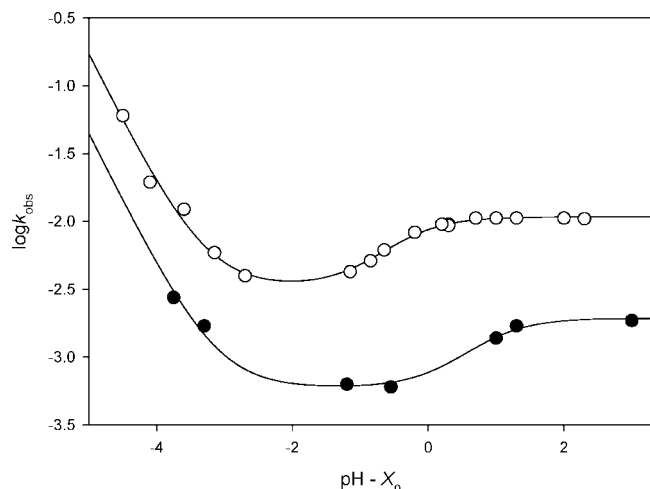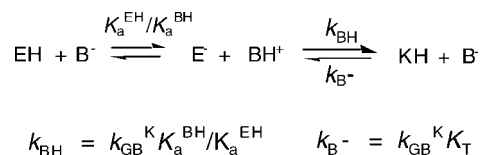
FIGURE 3. Plot of $\log k_{obs}$ against $pH - X_o$ for the ketonization of phenylacetylpyrazine enol at 25 °C: upper curve H_2O-HCl; lower curve, D_2O-DCl.

(or D_3O^+) following ionization of the enol to its enolate anion.[21] An isotope effect can also be evaluated for the dissociation constant corresponding to the increase in initial absorbance at $\lambda_{max} = 395$ nm in the concentration range 0.01–1 M DCl. In HCl as in $HClO_4$ this was ascribed to conversion of the protonated to unprotonated phenylacetylpyrazine enol (cf. eq 8). Values of pK_a were determined from intital absorbances recorded in Table S10 (Supporting Information) as 0.42 ± 0.05 and 1.00 ± 0.1 in H_2O and D_2O respectively, which give a solvent isotope effect on the protonation equilibrium of $K_a^{H2O}/K_a^{D2O} = 3.8$. As described above, this solvent isotope effect was taken into account when correcting NMR measurements of the pK_a for the protonated keto tautomer from D_2O to H_2O. It is less easy to evaluate accurately an isotope effect for the "chloride ion-catalyzed" reaction, but the calculated pH profiles yield an approximate value of $k_{H2O}/k_{D2O} = 4$. Both pH and pD profiles also imply a second acid-independent reaction at high acidities prior to the onset of the chloride ion-promoted reaction with approximate rate constants $k_{H2O} = 3.3 \times 10^{-3}$ s^{-1} and $k_{D2O} = 6.4 \times 10^{-4}$ s^{-1} and hence a further large solvent isotope effect $k_{H2O}/k_{D2O} = 5$, which is again consistent with a pre-equilibrium deprotonation, this time of the protonated enol, followed by rate-determining protonation (of the enol) by H_3O^+. However, a discrepancy between the rate constant in H_2O/HCl and $k_{H2O} = 1.51 \times 10^{-3}$ s^{-1} from aqueous $HClO_4$ suggests that this value may not be accurately estimated from the pH profile for HCl (Figure 3) and that this isotope effect is overestimated.

Enolization Reaction. In addition to the ketonization reaction, rate constants were measured for the reactions of iodine and bromine with the keto tautomer of phenylacetylpyrazine. In the presence of a large excess of the ketone and at not too high acid concentrations (for the iodination) the halogenation reactions were zero order in halogen and first order in ketone. The iodine and bromine were complexed with excess iodide or bromide ions and the reactions were monitored spectrophotometrically from depletion of I_3^- and Br_3^-, respectively, as the halogenations progressed. The reaction was subject to general base catalysis in acetic acid buffers, and measured first-order rate constants for these buffers are contained in Table S11 (Supporting Information). Table S12 (Supporting Information) contains rate constants for bromination in dilute perchloric acid solutions Bromination in dilute solutions of perchloric acid showed mild acid catalysis and a pH-independent reaction with

SCHEME 1

$$EH + B^- \underset{}{\overset{K_a^{EH}/K_a^{BH}}{\rightleftharpoons}} E^- + BH^+ \underset{k_{B^-}}{\overset{k_{BH}}{\rightleftharpoons}} KH + B^-$$

$$k_{BH} = k_{GB}{}^K K_a{}^{BH}/K_a{}^{EH} \qquad k_{B^-} = k_{GB}{}^K K_T$$

rate constant 1.37×10^{-5} s^{-1}, close to the average of those determined from iodination (1.27×10^{-5}).

The independence of measured rate constants of the nature of the halogen (bromine or iodine) and their dependence upon the concentrations of halide ions, substrate, and acetate buffer, as well as upon pH, are consistent with their expected correspondence to the enolization of phenylacetylpyrazine. This interpretation is confirmed insofar as the ratios of rate constants for halogenation and ketonization measured under similar conditions gave consistent values of $K_T = 1.20 \times 10^{-3}$ and 1.10×10^{-3} for the acetate-catalyzed and uncatalyzed reactions respectively which may be identified as the keto–enol tautomerisation constant for the reaction. As described below a further value of $K_T = 1.50 \times 10^{-3}$ was obtained from the ratio of rate constants for iodination and ketonization catalyzed by zinc ions. The average of these values is 1.27×10^{-3}.

The observation of acid catalysis of bromination in dilute perchloric acid solutions was surprising because the measured rate constant (3.8×10^{-4} s^{-1}) was too large to be consistent with an acid-catalyzed enolization. Because a faster acid-catalyzed bromination was found for pyrazine itself (i.e. **1** lacking the $PhCH_2CO$ group) it seems likely that this represents bromination of the ring. However, no attempt was made to isolate a product, and investigation of the reaction was not pursued. Bromination of pyrazine in the absence of acid was not observed.

Microscopic Rate Constants. The rate constants measured for enolization and ketonization reactions catalyzed by hydrogen ions, hydroxide ions, and buffer bases (eq 2) can be dissected into microscopic values k_{BH} and k_{B^-} for protonation of the enolate anion by an acid (BH) or proton abstraction from the keto form of phenylacetylpyrazine by a base (B^-). These rate constants are shown in Scheme 1. They are related to the rate constant $k_{GB}{}^K$ for (general) buffer base-catalyzed ketonization by equations (also included in Scheme 1) in which $K_a{}^{BH}$ and $K_a{}^{EH}$ are ionization constants for the buffer acid and enol of phenylacetylpyrazine respectively.[3]

The equations need a little adaptation when BH is H_3O^+ or H_2O. Thus, for H_3O^+, $k_{BH} = k_{H2O}{}^K K_a{}^{EH}$ and $k_{B^-} = k_{H2O}{}^K K_T$, where $k_{H2O}{}^K$ is the rate constant for the uncatalyzed ketonization of the enol. For H_2O, $k_{B^-} = k_{OH}{}^K$, the directly measured rate constant for ionization of phenylacetylpyrazine to its enolate anion, and $k_{BH} = k_{OH}{}^K K_w/K_a{}^{EH}$.

Values of k_{BH} and k_{B^-} for H_3O^+, acetic acid, lutidinium ion, and water are listed in Table 2. Although measurements were also made in borate buffers, the catalysis was quite weak and the values of $k_{GB}{}^K$ (eq 2) from Table 2 were not deemed accurate enough for calculation of microscopic rate constants.

In principle, microscopic rate constants may be derived also from enolization measurements. Thus, the rate constant $k_{GB}{}^E$ for acetate-catalyzed enolization of phenylacetyl pyrazine corresponds to k_{B^-} (Scheme 1), and the same is true of the uncatalyzed reaction (with water as the base). In practice, the magnitude of these values is taken into account in deriving average values for the relevant k_{B^-} and k_{BH} rate constants in

TABLE 2. Microscopic Rate Constants for the Ionization of Phenylacetylpyrazine to its Enolate Anion (k_{B^-}) and the Reverse Protonation of the Enolate Anion (k_{BH})

|	H_3O^+	AcOH	lutidine	H_2O
pK_a	−1.76	4.78	6.69	15.76
$k_{BH}{}^a$	1.19×10^7	3.20×10^4	4.90×10^3	0.33
$k_{B^-}{}^b$	1.51×10^{-5}	2.46×10^{-3}	0.030	40.5

[a] Rate constant for protonation of the enolate anion by indicated acid. [b] Rate constant for proton abstraction from phenylacetylpyrazine by conjugate base of indicated acid.

Table 2. The values in Table 2 are also consistent with averaged measurements of the tautomeric constant K_T.

One further microscopic rate constant may be identified in connection with the H^+-catalyzed ketonization of the enol implied in eq 8. The measured rate constant is 1.51×10^{-3} s^{-1} and refers to the pH-independent reaction in the perchloric acid concentration range 4−9 M. This is interpreted as a reaction of the monoprotonated enol in which the rate-determining step involves protonation by H_3O^+ of either the neutral enol or, as is observed for 2-phenylacetylpyridine, its zwitterionic tautomer **10**. The rate constant for reaction of an acid with the neutral enol (or zwitterion) is denoted k_{AH} by analogy with k_{BH} for reaction with its conjugate base. If the enol is the reactive intermediate, $k_{AH} = 1.51 \times 10^{-3}/K_a^{EH2+} = 4.16 \times 10^{-3}$ based on the (averaged) value of 0.44 for pK_a^{EH2+}.

It is now possible to evaluate a rate constant k_{A^-} for the reverse reaction of protonated ketone with water based on eqs 10 and 11. Taking the ionization constant of the N-protonated ketone pK_a^{KH2+} as −0.90 and K_T as 1.27×10^{-3} gives $k_{A^-} = 4.20 \times 10^{-5}$. The magnitude of this rate constant does not depend on whether it is the enol or zwitterion which undergoes protonation in the ketonization direction. However, if it is the zwitterion which is subject to protonation k_{AH} will be modified by the equilibrium constant between the zwitterion and the enol. An attempt to estimate this equilibrium constant is described below.

$$EH + H_3O^+ \underset{k_{A^-}}{\overset{k_{AH}}{\rightleftharpoons}} KH_2^+ + H_2O \overset{K_a^{KH2+}}{\rightleftharpoons} KH + H_3O^+ \quad (10)$$
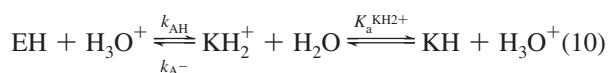
$$k_{A^-} = k_{AH}K_a^{KH2+}K_T \quad (11)$$

Correlation of pK_a Values for Substituted Pyridines and Pyrazines. An equilibrium constant for interconversion of the enol **8** and zwitterion **10** tautomers of phenylacetylpyrazine could be derived if a pK_a for N-protonation of the enolate anion to form the zwitterion was known. This pK_a cannot be measured directly but it may be estimated from corresponding values for 2- and 3-phenylacetylpyridines and a correlation between pK_a values of substituted pyridines and pyrazines.

This correlation is complicated by the presence of alternative sites for protonation of the pyrazine. For a substituted pyrazine, the substituent is situated in a 2-position with respect to the 1-nitrogen atom and a 3-position with respect to the 4-nitrogen atom (**12**). The experimental pK_a is then an apparent value (pK_a^{app}) related to the pK_a values for the individual positions by eq 12 in which the superscripts −1 and −4 for K_a indicate protonation at the 1- and 4-nitrogens, respectively.

$$1/K_{app} = 1/K_a^{-1} + 1/K_a^{-4} \quad (12)$$

TABLE 3. pK_a Values for 2- and 3-Protonation of Substituted Pyrazines[a] and for Protonation of 2- and 3-Substituted Pyridines in Aqueous Solution at 25 °C

substituent	$pK_{app}{}^b$	pK_a (pyridine)	$\Delta pK_a{}^c$	pK_a (pyrazine)
H	0.8	5.17	0	0.5
2-CH$_3$	1.45	5.97	0.29	1.27
3-CH$_3$	1.45	5.68	0.29	0.98
2-PhCOCH$_2$	0.40	5.03	0.16	0.17
3-PhCOCH$_2$	0.40	4.87	0.16	0.01
2-CH$_3$CO	−0.90	2.30	−1.13	−2.00
3-CH$_3$CO	−0.90	3.43	−1.13	−0.87
2-PhCH$_2$CO	−0.90	2.30	−0.29	−1.37
3-PhCH$_2$CO	−0.90	2.59	−0.29	−1.08
2-PhCH=C(OH)	0.50	4.0	−0.10	0.15
2-PhCH=C(OH	0.50	4.1	−0.10	0.25
2-CH$_3$O	0.75	3.28	−1.60	−0.86
3-CH$_3$O	0.75	4.88	−1.60	0.74
2-CH$_3$S	0.48	3.59	−0.83	−0.41
3-CH$_3$S	0.48	4.42	−0.83	0.42
2-NH$_2$	3.14	6.71	0.68	2.96
3-NH$_2$	3.14	6.03	0.68	2.38

[a] Derived as described in the text from values of pK_{app}. [b] Values of pK_{app} for protonation of substituted pyrazines; data from refs 4 and 23 or this study. [c] The difference in pK_a values of 2- and 3-substituted pyridines are assumed to be the same for 2- and 3-protonation of the correspondingly substituted pyrazine; data from refs 2, 5, and 23.

If we assume that the difference in pK_a values at the two positions, ΔpK_a, is 0.9 times the difference in pK_a values of the corresponding 2- and 3-substituted pyridines (**13** and **14**), then we can infer individual pK_a values for the pyrazine nitrogen atoms from the measured value of pK_a^{app} by combining eq 12 with eq 13 (for 2- and 3-substituted pyridines) to obtain eqs 14 and 15. The multiplication by 0.9 is based on the slope of the plot of pK_a values of pyrazines against pK_a values of pyridines obtained below.

12 **13** **14**
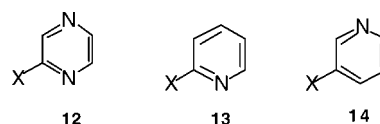
$$pK_a^{-2} - pK_a^{-3} = \Delta pK_a \quad (13)$$

$$pK_a^{-4} = pK_a^{app} - \log(1 + 10^{0.9\Delta pK_a}) \quad (14)$$

$$pK_a^{-1} = pK_a^{-4} + 0.9\Delta pK_a \quad (15)$$

Values of pK_a^{-1} and pK_a^{-4} derived in this way are listed in Table 3 together with pK_a values for the corresponding 2- and 3-substituted pyridines.[23] For phenylacetylpyrazine itself, for example, $pK_{app} = -0.9$ was combined with pK_a values 2.30 and 2.59, respectively, for the 2- and 3-phenylacetylpyridines ($\Delta pK_a = -0.29$) to derive $pK_a^{-1} = -1.35$ and $pK_a^{-4} = -1.09$ for the 1- and 4-nitrogen atoms. The correlation between pK_a values of pyrazines and pyridines is shown in Figure 4, with values of pK_a^{-1} plotted against the pK_a values of 2-substituted pyridines and values of pK_a^{-4} plotted against pK_a values of 3-substituted pyridines. The correlation shows considerable scatter, but the best straight line through the points yields the following relationship.

(23) Jencks, W. P.; Regenstein, J. *Handbook for Biochemistry*, 2nd ed.; Sober, H. A., Harte, H. J., Eds.; Chemical Rubber Co.: Cleveland, OH, 1970; pp J187−226.

$$pK_a^{\text{pyradine}} = (0.90 \pm 0.08)pK_a^{\text{pyradine}} - 3.70 \pm 0.37 \tag{16}$$

Zwitterion Tautomers of Phenylacetylpyrazine. As noted above, the required pK_a values for loss of a proton from the 1- and 4-zwitterionic tautomers of phenylacetylpyrazine to yield enolate anions may be inferred from the correlation of Figure 4 and knowledge of the pK_a values of the zwitterionic isomers of phenylacetylpyridine. The pK_a values for the latter ions may be derived from measurements of pK_a values for the deprotonation of the corresponding *N*-methylphenylacetylpyridinium ions corrected for replacement of the *N*-hydrogen atom by a methyl group.[7] The dissociation eqilibrium is shown for the 2-substituted cation below.

$$\tag{17}$$
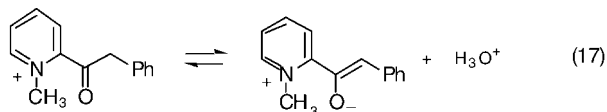
Substitution of pK_a values of 5.9 and 7.4 for the 2- and 3-phenylacetylpyridine zwitterions[7] in eq 16 yields 2.9 and 1.6 as the corresponding values for the 1- and 4-*N*-protonated phenylacetylpyrazine zwitterions. The tautomeric constants (pK_T) for interconversion of enol and 1- and 4-zwitterions can then be obtained as 6.1 and 7.4, respectively, based on the thermodynamic cycles of Scheme 2, which include the known ionization constant of the enol ($pK_a = 9.0$). In Scheme 2, the double arrows for equilibria are replaced by single arrows to indicate the direction of reaction to which the equilibrium constant refers.

These equilibrium constants for the zwitterions allow construction of "complete" networks of equilibrium constants for the ionization and tautomerisation of phenylacetylpyrazine as described in the Discussion.

Catalysis of Tautomerization by Metal Ions. The ease with which the ketonization reaction could be monitored and the absence of competing acid catalysis (except at high acid concentrations) provide favorable conditions for the study of catalysis by metal ions. First-order rate constants for reaction of Cu^{2+}, Ni^{2+}, Co^{2+}, Zn^{2+}, and Cd^{2+} ions were measured in aqueous solutions of 0.1 M HCl. The rate constants are listed
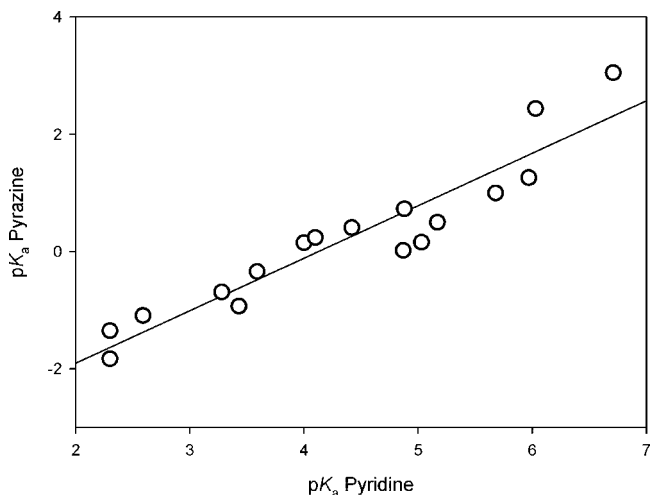
FIGURE 4. Plots of "dissected" pK_a values for the protonation at 1- and 4-positions of 2-substituted pyrazines against pK_a values of corresponding 2- and 3-substituted pyridines.
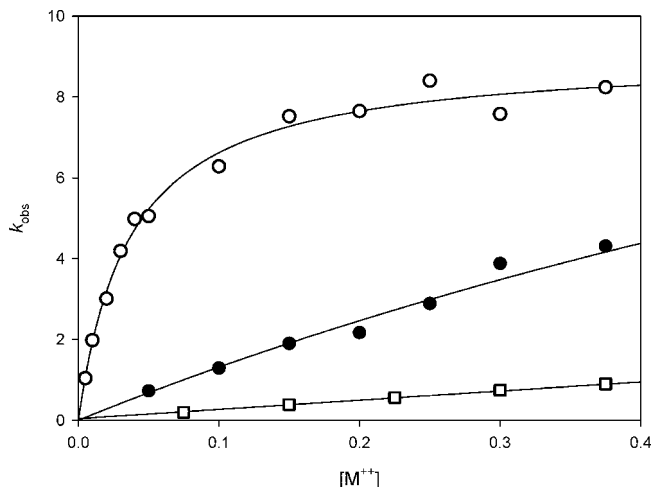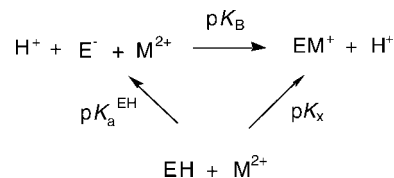
FIGURE 5. Plots of k_{obs} for the ketonization of phenylacetylpyrazine enol in 0.1 M $HClO_4$ against concentrations of metal ions in aqueous solution at 25 °C.

SCHEME 2
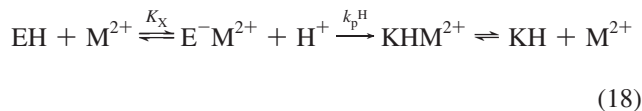
1-protonated zwitterion   4-protonated zwitterion
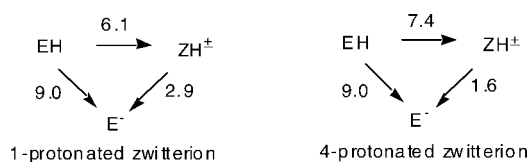
SCHEME 3

in Table S13 (Supporting Information) and are plotted against the concentrations of metal ions for Cu, Ni, and Zn in Figure 5. For all the ions except Cu^{2+} the plots are linear or nearly linear, and second-order rate constants may be derived from their (limiting) slopes. These constants (k_M^K) are listed in Table 4 where they are compared with the second-order rate constant for catalysis by hydrogen ions and first-order rate constant for the uncatalyzed reaction. Also shown in Table 4 are rate constants for the reverse metal ion-catalyzed enolization reactions (k_M^E) obtained by combining the rate constants for ketonization with the equilibrium constant for tautomerisation, $K_T = 1.27 \times 10^{-3}$.

In Figure 5 it can be seen that catalysis by Cu^{2+} ions is subject to kinetic saturation. This may be interpreted in terms of a reaction scheme (eq 18) in which a metal bound enolate anion (E^-M^{2+}) reacts with H_3O^+ to yield the coordinated ketone.[6] Formation of the metal−enolate complex involves exchange of an enolic hydrogen atom for a metal ion. Saturation occurs as the direction of this equilibrium shifts from left to right. The observed kinetic behavior can be formulated in terms of the equilibrium constant for the exchange reaction (K_x), the rate constant for protonation (k_p) and the concentration of metal ion as in eq 19. At high concentrations of metal ion the limiting first order rate constant $k_{max} = k_p^H[H^+]$. At low concentrations of metal ion the limiting second-order rate constant $k_M = k_p^H K_x$. The metal ion concentration at half-maximal rate corresponds to an apparent binding constant $K_{app} = K_x/[H^+]$.

$$\text{EH} + \text{M}^{2+} \overset{K_X}{\rightleftharpoons} \text{E}^-\text{M}^{2+} + \text{H}^+ \xrightarrow{k_p^H} \text{KHM}^{2+} \rightleftharpoons \text{KH} + \text{M}^{2+}$$
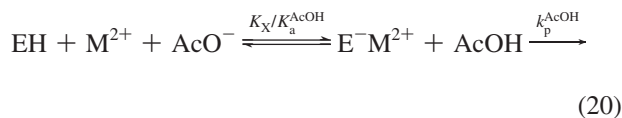
(18)

$$k_{obs} = \frac{k_p^H[\text{H}^+]}{(1 + [\text{H}^+]/K_X[\text{M}^{2+}])}$$

(19)

A best fit of eq 19 to the data for catalysis by Cu^{2+} gives k_p^H = 90.5 M^{-1} s^{-1} and $K_x = 2.72 \pm 0.23$. The limiting value of k_{obs} at high concentrations of metal ion, k_{max}, corresponds to $k_p^H[\text{H}^+] = 9.05$ s^{-1}. The limiting slope of the plot of k_{obs} against $[\text{M}^{2+}]$ gives $k_pK_x = 246$ M^{-1} s^{-1}. The latter value represents the second order rate constant (k_M^K) for catalysis of ketonization by Cu^{2+} ions shown in Table 4.

Catalysis by zinc ions was also studied in 0.02 M 1:1 acetic acid buffers (ionic strength 1.17). At this pH, the zinc catalysis is also subject to strong saturation. The rate constants are listed in Table S14 (Supporting Information). They yield a value of $k_{max} = 1.17$ s^{-1} and apparent binding constant for zinc ions K_{app} = 18.9 $\pm$ 2.5.

For acetic acid buffers, the reaction scheme in eq 18 is modified to that in eq 20 in which the metal−enolate complex is now protonated by acetic acid instead of H_3O^+. Equation 19 is unchanged except that $k_p^H[\text{H}^+]$ in the numerator is replaced by $k_p^{AcOH}[\text{AcOH}]$, as shown in eq 21.

$$\text{EH} + \text{M}^{2+} + \text{AcO}^- \overset{K_X/K_a^{AcOH}}{\rightleftharpoons} \text{E}^-\text{M}^{2+} + \text{AcOH} \xrightarrow{k_p^{AcOH}}$$

(20)

$$k_{obs} = \frac{k_p^{AcOH}[\text{AcOH}]}{(1 + [\text{H}^+]/K_X[\text{M}^{2+}])}$$

(21)

Identifying k_{max} with $k_p^{AcOH}[\text{AcOH}]$ gives a value of k_p^{AcOH} = 58.5 M^{-1} s^{-1}. As before, the apparent binding constant for zinc ions K_{app} corresponds to $K_x/[\text{H}^+]$, and this implies a value of $K_x = 4.64 \times 10^{-4}$ (taking $pK_a^{AcOH} = 4.61$ at the prevailing ionic strength of 1.17). The limiting second order rate constant at low metal ion concentrations is $k_p^{AcOH}(K_x/[\text{H}^+])[\text{AcOH}]$ = 22.1 M^{-1} s^{-1} ([AcOH] = 0.02 M, pH = 4.55).

The exchange equilibrium constants K_x for copper and zinc ions are conveniently converted to equilibrium constants K_B for binding the metals to the enolate anion by making use of the thermodynamic cycle shown in Scheme 3. Again the equilibria

are represented by single arrows to show the directions of reactions to which the pKs refer.

From Scheme 3 it is apparent that $pK_B = pK_x - pK_a^{EH}$ (or $K_B = K_x/K_a^{EH}$) where $pK_a^{EH} = 9.0$ refers to the ionization constant of the enol tautomer of phenylacetylpyrazine. Values of binding constants are, however, more conveniently expressed as log K_B rather than pK_B because this yields positive rather than negative values and, in the case of the proton, log K_B = pK_a. For the zinc, copper and hydrogen ions values of log K_B are 5.66, 9.43, and 9.00, respectively. These values are also listed in Table 4.

In addition to ketonization, enolization catalyzed by zinc ions was studied in aqueous solution in the absence of buffers.[24] Measured first-order rate constants are listed in Table S15 (Supporting Information) and when plotted against metal ion concentration give a straight line with slope corresponding to a second order rate constant $k_M^E = 3.68 \times 10^{-3}$ M^{-1} s^{-1}. Combining this rate constant with the rate constant 2.46 M^{-1} s^{-1} for zinc-catalyzed ketonization in water yields $K_T = 1.50 \times 10^{-3}$ in good agreement, as we have seen, with values for other catalysts.

For enolization it was difficult to detect and measure the saturation of catalysis with increasing zinc ion concentration. However, the extent of curvature was increased by the addition of trifluoroethanol to the aqueous medium, and in a dilute cacodylate buffer in 60% v/v TFE−H_2O a value of K_B was measured as 6.9 M^{-1}. First order rate constants for iodination on which the measurement is based are listed in Table S16 (Supporting Information) and plotted against $[Zn^{2+}]$ in Figure S3 (Supporting Information). The third-order rate constant for zinc and cacodylate-catalyzed enolization in 60%TFE is 5.4 M^{-2} s^{-1}. In order to extrapolate the value of K_B to water, rate constants for the iodination of acetylpyridine catalyzed by zinc ions in 60% v/v TFE−H_2O in the absence of buffer were similarly measured, and a value of $K_B = 65.0$ was derived. Since a value of $K_B = 35.7$ M^{-1} had previously been measured in water,[24] it was assumed that enolization of phenylacetylpyrazine would be characterized by the same ratio of rate constants in water and 60% TFE as acetylpyridine. On this basis, K_B for binding of zinc ions to phenylacetylpyrazine in water is 6.9 $\times$ 35.7/65 = 3.8 M^{-1} and log K_B = 0.6. Rate constants for the zinc-catalyzed iodination of acetylpyridine in aqueous TFE are listed in Table S17 (Supporting Information).

**TABLE 4. Rate Constants and Binding Constants for Catalysis of Ketonization by Protons and Metal Ions in Aqueous Solution at 25 °C**

catalyst	acid[a]	$k_M^{K\,b}$	$k_M^{E\,c}$	$\log K_B{}^d$	$k_p^{e,f}$	$k_{-p}^{f,g}$
none	AcOH	1.94	2.46×10^{-3}	0	3.2×10^4	2.46×10^{-3}
none	H^+	1.19×10^{-2}	1.51×10^{-5}	0	1.19×10^7	1.51×10^{-5}
Cd^{2+}	H^+	0.31	3.94×10^{-4}			
Zn^{2+}	AcOH	22.1	2.81×10^{-2}	5.66	58.5	7.4×10^{-3}
Zn^{2+}	H^+	2.46	3.12×10^{-3}	5.66	5.30×10^3	5.6×10^{-4}
Co^{2+}	H^+	8.67	1.10×10^{-2}			
Ni^{2+}	H^+	11.0	1.40×10^{-2}			
Cu^{2+}	H^+	246.0	0.312	9.43	90.5	
H^+	H^+	4.16×10^{-3}	5.28×10^{-6}	9.00	4.16×10^{-3}	4.20×10^{-5}

[a] The acid protonating complexed (or for the uncatalyzed reactions uncomplexed) enolate anion in the ketonization reaction, with rate constant k_p. (In the reverse enolization, the conjugate base (H_2O or AcO^-) abstracts a proton from the complexed (or uncomplexed) ketone, with rate constant k_{-p}.) [b] Rate constant for catalyzed or uncatalyzed ketonization. [c] Rate constant for catalyzed or uncatalyzed enolization [d] Log K_b is the log of the binding constant of the metal ion or proton to the enolate anion. In the case of the proton it corresponds to the pK_a of the enol. [e] See footnote a; k_p corresponds to k_{BH} for uncatalyzed reactions and k_{AH} for the H^+-catalyzed reaction. [f] There are no values for metal ions for which binding constants were not determined; for Zn^{2+}, $K_B = 3.8$ M^{-1}. [g] See footnote a; k_{-p} corresponds to k_{A^-} for the H^+-catalyzed reaction and k_{B^-} for the uncatalyzed reactions.

SCHEME 4

SCHEME 5
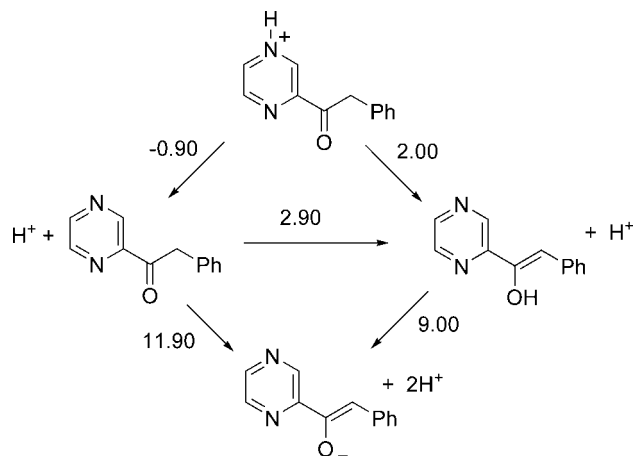
Discussion

Equilibrium Constants for Ionization and Tautomerization. The pK_a values for ionization of phenylacetylpyrazine in base and acid are readily measured as 11.90 and -0.90, respectively. The value in acid includes a correction for a solvent isotope effect upon the value measured as -0.40 in D_2O. That the ionization occurs in dilute solutions of base means that the less stable enol tautomer can be generated by quenching the enolate anion in excess acid or acidic buffer.[2−5] Rates of relaxation of the enol to form the keto tautomer may then be monitored spectrophotometrically. The reverse enolization reaction can be monitored by iodination or bromination of the ketone. Combining rate constants for the two reactions yields an equilibrium constant for tautomerisation K_T = [enol]/[ketone] = 1.27×10^{-3} and pK_T = 2.90. This constant can be combined with the ionization constants for the ketone to yield additional ionization constants for the enol tautomer based on the thermodynamic cycles of Scheme 4 (in which, again, the arrows indicate directions of reaction to which the equilibrium constants refer).

The site of protonation of the pyrazine ring in Scheme 4 is shown as the nitrogen atom at the 4-position. In practice, pK_a values for 2- and 3-phenylacetylpyridine of 2.30 and 2.59, respectively, and for 2- and 3-acetylpyridine of 2.30 and 3.43, suggest that although protonation should occur predominantly at this position there may be a significant contribution from protonation at the 1-position. As described above, the pK_a = -0.90 may be treated as an apparent value implying pK_a values of -1.35 and -1.1 for the 1- and 4-nitrogen atoms respectively, based on the difference in pK_a values of the 2- and 3-phenylacetylpyridines. The dissected pK_a values indicate that there is twice as much protonation at the 4- than 1-position.

pH Profile. Rate constants for relaxation of enol or ketone reactants are shown as a plot of log k against pH in Figure 2. In aqueous sodium hydroxide the reaction corresponds to ionization of the keto tautomer to its enolate anion. At lower pH, the enolate anion is quenched in media sufficiently acidic to effect its protonation, and the observed reaction is conversion of enol to keto tautomer. In concentrated $HClO_4$ inflections in the profile may be interpreted in terms of mono and diprotonation of the enol. From the acid dependence of associated absorbance changes pK_a values of 0.45 and -4.80 can be assigned. These values may be compared with 0.65[23] and
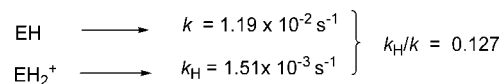
-6.25[25] reported for the protonation of pyrazine itself. The latter measurement represents H_o at half-protonation and is not strictly a pK_a. Nevertheless, the large difference from pK_a = -4.80 is consistent with a significant stabilization of the pyrazine dication by the enolic substituent, which is also suggested by strong conjugation between the two groups implied by the long wavelength of the principal UV−vis absorption (λ_{max} = 510 nm). It is a little surprising therefore that there appears not to be a complementary stabilization of the monoprotonated enol (pK_a = 0.44) which is of comparable acidity to the protonated pyrazine (pK_a = 0.5).

In aqueous buffers, the dependence of the rate constants upon buffer concentrations and pH is consistent with a base-catalyzed mechanism for tautomerisation, with the enolate anion as reactive intermediate. This corresponds to the lower pathway of Scheme 4 (if the direction of an arrow is reversed!). Below pH 7, the reaction is independent of pH and proceeds with initial ionization of the enol reactant followed by protonation of the enolate anion by H_3O^+ as in eq 22.

$$EH \rightleftharpoons E^- + H_3O^+ \rightarrow KH \qquad (22)$$
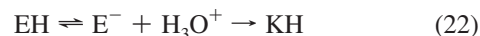
This reaction is retarded by acid. This is apparent from the form of the pH profile close to pH = 0 and at higher acidities. The downward inflection above pH = 0 corresponds, as we have seen, to protonation of the enol with pK_a = 0.44. The decrease in rate at pHs below this pK_a represents inhibition of the reaction by acid. At higher acid concentrations the reaction again becomes pH independent, and this must represent the H^+-catalyzed reaction of the enol, albeit with the protonated enol as reactant.

It is unusual for keto−enol tautomerization to be inhibited by acid. The extent of the inhibition is expressed by the ratio of first-order rate constants for neutral and protonated enols as reactants in Scheme 5.

In the reverse direction (enolization), the protonated ketone is indeed more reactive than the unprotonated ketone, but the difference is small: 3.8×10^{-5} s^{-1} compared with 1.52×10^{-5} s^{-1}. This reversal of reactivities occurs because K_T for tautomerisation of keto to enol tautomers is larger for the protonated than unprotonated enol, i.e., pK_T = 1.57 compared with 2.90 (see below).

O- versus N-Protonation. As with phenacylpyrazine (**5**), the following dilemma arises: does acid-catalyzed enolization proceed with protonation of the keto tautomer at a nitrogen atom or oxygen atom? In other words, is there a zwitterionic intermediate on the pathway from enol to protonated ketone, as shown in eq 8? Factors favoring conversion of the enol to a zwitterion prior to protonation have been discussed elsewhere.[4] As outlined in the Supporting Information, it is difficult to say whether this is true of phenylacetylpyrazine. If the reaction does not proceed with N-protonation, phenylacetylpyrazine is the first heterocyclic ketone studied for which this has been found to

(24) Cox, B. G. *J. Am. Chem. Soc.* **1974**, *96*, 6823–6828.
(25) Brignell, P. J.; Johnson, C. D.; Katritzky, A. R. *J. Chem. Soc. B* **1967**, 1233–1237.
(26) Alunni, S.; Del Giacco, T.; De Maria, P.; Fifi, G.; Fontana, A.; Ottavi, L.; Tesei, I. *J. Org. Chem.* **2000**, *69*, 3276–3281.
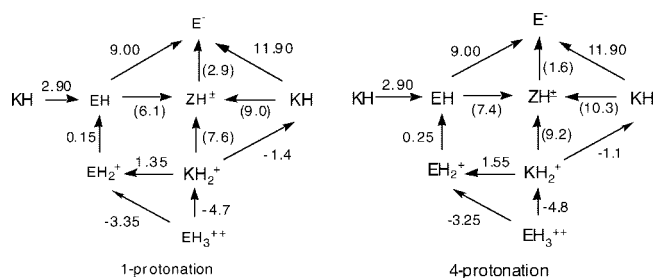
SCHEME 6

1-protonation

4-protonation

TABLE 5.   Ratios of Rate Constants for Catalyzed and Uncatalyzed Enolization of Phenylacetylpyrazine for Proton and Metal Ion Catalysts with Water as Base

	H^+	Cd^{2+}	Zn^{2+}	Co^{2+}	Ni^{2+}	Cu^{2+}
k_M/k_o (l mol^{-1})	0.35	26.0	207	729	924	20,700

be true. If it does, then the *O*-protonation route must be deemed unusually slow.

Networks of Equilibrium Constants. Dissection of apparent equilibrium constants for the acid ionization of phenylacetylpyrazine and inclusion of estimates of pK_a values for zwitterionic tautomers allows expansion of Scheme 4 into more comprehensive networks of equilibrium constants referring, respectively, to protonation at the 1- and 4-nitrogen atoms of the ring, as shown in Scheme 6. Note that the distinction between positions of protonation applies only to species protonated at nitrogen, namely KH_2^+, EH_2^+ and $ZH^\pm$. As already mentioned, in Scheme 4 the $pK_a = -0.90$ for *N*-protonation of phenylacetylpyrazine is an apparent value which may be separated into pK_a values of -1.4 and -1.1 for 1- and 4-protonation by assuming that the ratio of the two ionization constants is the same as for protonation of 1- and 4-phenylacetyl pyridines. Also included in Scheme 6 are pK_a values for mono and diprotonation of the phenylacetylpyrazine enols.

The format of Scheme 6 follows that used for other heterocyclic ketones.[2,4,5] Acid dissociation equilibria are indicated by vertical or diagonal arrows and tautomeric equilibria by horizontal arrows. The numbers in brackets are for equilibria involving the zwitterion tautomers for which the equilibrium constants are based on the correlation between pK_a values of correspondingly substituted pyrazines and pyridines (Figure 4).

Metal Ion Catalysis. The weak catalysis of tautomerization of phenylacetylpyrazine by acid means that catalysis by metal ions is readily observable. Partly as a consequence, catalysis by metal ions is considerably more effective than by protons. This is apparent from Table 5, which compares ratios of rate constants (k_H/k_o or k_M/k_o) for catalyzed and uncatalyzed ketonization reactions. The ratios represent the acceleration produced by an (ideal) one molar concentration of catalyst. Unusually, rate constants for the acid-catalyzed reactions are smaller than for the uncatalyzed reactions (for water or acetate ions acting as bases). Correspondingly, ratios of rate constants for metal ion-catalyzed to proton-catalyzed reactions are high: e.g., $k_{Zn}/k_H = 591$ and $k_{Cu}/k_H = 58600$.

There have been a number of investigations of the relative effectiveness of protons and metal ions in Lewis acid catalyzed reactions. Preliminary results for tautomerization of phenacyl- and phenylacetyl-pyridines and also phenacylpyrazine have been reported by ourselves,[6] and an extensive range of enolization reactions has been investigated by Fontana and De Maria.[18] Other reactions studied or reviewed recently include eliminations

SCHEME 7
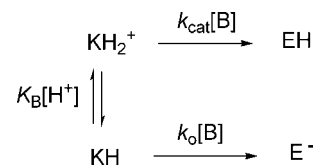
SCHEME 8
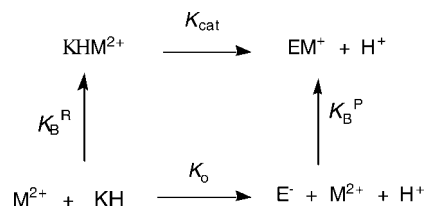
activated by a β-pyridyl substitutent,[26] bromination of keto-amides,[27] hydrogen isotope exchange of nucleotide bases,[28,29] and a zinc-catalyzed hydride rearrangement.[30] In this paper, we focus on the difference between the ketonization of phenyl-acetylpyrazine **1**, which appears to be characterized by the largest metal ion-to-proton rate ratio so far recorded, and the apparently structurally similar phenacylpyridine **2** for which an even larger difference in rates is observed,[6] but now with the proton more rather than less effective than the metal ion, i.e., $k_H/k_{Zn} = 1600$.

To understand the marked contrast between these two substrates it is helpful to represent the catalysis within the conventional framework of Scheme 7, which shows uncatalyzed and H^+-catalyzed reaction pathways for enolization.[31] Enolization indeed is the reverse of the ketonization reactions considered above, but the magnitude of the catalysis is unchanged by the direction of reaction. In the enolization direction, the uncatalyzed reaction involves transfer of a proton from the methylene group of the ketone to a base B (which in the examples just considered is the solvent water) to form an enolate anion (E^-). In the catalyzed reaction the proton is initially bound to the substrate with equilibrium constant K_B and the protonated substrate then reacts with rate constant k_{cat} to give the enol (EH). A similar scheme applies to catalysis by metal ions. The binding constant corresponds to the inverse of the dissociation constant for the substrate–catalyst complex (KH_2^+) and for catalysis by H^+ log $K_B = pK_a$.

From Scheme 7 it is evident that the ratio of rate constants for catalyzed and uncatalyzed reactions (k_H/k_o) corresponds to $K_B(k_{cat}/k_o)$. This ratio has been designated the "proficiency" of a catalyst by Wolfenden.[32] As noted above, it corresponds to the acceleration of the uncatalyzed reaction produced by one molar concentration of catalyst (although this acceleration is realized only when the solute is less than fully complexed, i.e., when [catalyst] > $1/K_B$).

The importance of $K_B(k_{cat}/k_o)$ is emphasized by its wide interpretation as an equilibrium constant for binding a catalyst

(27) Hynes, M. J.; Clarke, E. M. *J. Chem. Soc. Perkin Trans. 2* **1998**, 1263–1267.
(28) Jones, J. R.; Taylor, S. E. *J. Chem. Soc. Perkin Trans. 2* **1979**, 1773–1776.
(29) Buncel, E.; Clement, O.; Onyido, I. *Acc. Chem. Res.* **2000**, *33*, 672–678.
(30) Crugeiras, J.; Richard, J. P. *J. Am. Chem. Soc.* **2004**, *126*, 5164–5173.
(31) Hay, R. W. In *Comprehensive Coordination Chemistry*; Wilkinson, G., Gillard, R. D., McCleverty, J. A., Eds.; Pergamon Press: Oxford, 1987; Vol. 6, pp 411–485.
(32) Miller, B. G.; Wolfenden, R. *Annu. Rev. Biochem.* **2002**, *71*, 847–885.

to the transition state of an uncatalyzed reaction.[6,32−38] We will return to this point but focus first on the expression of k_H/k_o as the product of a binding constant (K_B) and rate constant ratio (k_{cat}/k_o). The ratio (k_{cat}/k_o) has been called by Stewart and Srinivasan a "proton activating factor" or "paf".[39] By analogy, for metal ion catalysis, k_{cat}/k_o becomes a metal-activating factor "maf".[40] De Maria and Fontana have referred to $K_B(k_{cat}/k_o)$ itself as a metal activating factor,[18] but in this paper we follow the usage of Stewart and Srinivasan

A Rate−equilibrium Relationship for Catalysis. If k_{cat}/k_o is considered a kinetic activating factor, it is convenient to identify an equilibrium activating factor, represented by the ratio of equilibrium constants for reaction of the bound and unbound substrates, which we may denote K_{cat}/K_o.[6] The magnitude of K_{cat}/K_o measures the increased thermodynamic driving force for reaction conferred by binding the catalyst. A relationship between kinetic and equilibrium factors can then be based on the Bronsted relationship between rate and equilibrium constants, $\log k_1/k_2 = \alpha \log K_1/K_2$, in which the coefficient α normally lies between 0 and 1. This relationship is shown in eq 23 and expresses the kinetic effect of the thermodynamic advantage arising from binding the catalyst.

$$k_{cat}/k_o = (K_{cat}/K_o)^\alpha \qquad (23)$$

A simple extension of eq 23 allows k_H/k_o or k_M/k_o ($= K_B k_{cat}/k_o$) to be expressed in terms of the binding constant for the catalyst-substrate complex and the equilibrium constant ratio K_{cat}/K_o as shown.

$$K_B k_{cat}/k_o = K_B(K_{cat}/K_o)^\alpha \qquad (24)$$

This equation is conveniently transformed by expanding Scheme 7 to include binding constants for the reactant and product (K_B^R and K_B^P) and replacing rate constants by equilibrium constants to form the thermodynamic cycle of Scheme 8.[6] In Scheme 8, the proton catalyst has been replaced by a metal ion (M^{2+}) and again the single arrows represent equilibria.
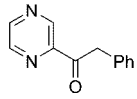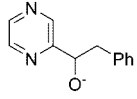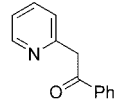
From Scheme 8 it is evident that $K_{cat}/K_o = K_B^P/K_B^R$. Making this substitution in eq 24 we obtain eq 25, in which the effectiveness of the catalysis is expressed in terms of equilibrium constants for binding the catalyst to reactants and products, the relative influence of which is determined by the Bronsted coefficient α.

$$K_B^R k_{cat}/k_o = K_B^R(K_B^P/K_B^R)^\alpha = (K_B^R)^{1-\alpha}(K_B^P)^\alpha \quad (25)$$

If the value α is approximated as 0.5 we obtain the following simple expression which allows the kinetic effect of the catalyst to be estimated solely from knowledge of the binding constants.

$$K_B^R k_{cat}/k_o = (K_B^R K_B^P)^{0.5} \qquad (26)$$

(33) Tee, O. S. *Adv. Phys. Org. Chem.* **1994**, *29*, 1–85.
(34) Kurz, J. L. *Acc. Chem. Res.* **1972**, *5*, 1–9.
(35) Kraut, J. *Science* **1988**, *242*, 533–540.
(36) Schneider, M. J.; Gaunitz, S.; Ridgeway, C.; Short, S. A.; Wolfenden, R. *Biochemistry* **2000**, *39*, 9746–9753.
(37) Schowen, R. L. *Transition States of Biochemical Processes*; Schowen, R. L., Gandour, R. L., Eds,; Plenum Press: New York, 1978; pp 77−117.
(38) Fersht, A. R. *Structure and Mechanism in Protein Science*, 3rd ed.; W H. Freeman and Co.: New York, 1998. Anslyn, E.; Dougherty, D. *Modern Physical Organic Chemistry*; University Science Books: Sausalito, 2005.
(39) Stewart, R.; Srinivasan, R. *Acc. Chem. Res.* **1978**, *11*, 271–277.
(40) Jones, J. R.; Taylor, S. E. *Chem. Soc Rev.* **1981**, 329–344.

TABLE 6. Binding Constants to Ketone and Enolate Anion and Calculated and Observed Rate Constant Ratios for Catalysis of Keto−Enol Tautomerization of Phenylacetylpyrazine and Phenacylpyridine by Zinc Ions and Protons in Aqueous Solution at 25 °C[a]

			$\frac{(\Delta pK_a^R + \Delta pK_a^P)^b}{2}$	$\log(k_H/k_{Zn})$
pK_a^H	-1.4[c]	2.9[c]		
			-2.33	-2.76
pK_a^{Zn}	0.6	5.56		
pK_a^H	5.03	12.22		
			3.86	4.04
pK_a^{Zn}	1.65	7.87		

[a] Binding constants from this work for phenylacetylpyrazine and ref 6 for phenacylpyridine. [b] The R (reactant) refers to the ketone and P (product) to the enolate anion; ΔpK_a corresponds to $pK_a^{Zn} - pK_a^H$ and $(\Delta pK_a^R + \Delta pK_a^P)/2$ represents values of $\log(k_H/k_{Zn})$ predicted from eq 28. [c] The pK_a for protonation at the 1-position of the pyrazine ring.

The approximation is an effective one partly because α is often not far from 0.5[4] and partly because when K_B^R and K_B^P are comparable in magnitude $K_B^R k_{cat}/k_o$ becomes insensitive to α. Failure of the relationship may signal an anomalous value for the Bronsted coefficient.

For proton catalysis we recognize that the binding constants for the catalyst are reciprocals of acid dissociation constants. If we replace $K_B^R k_{cat}/k_o$ by k_H/k_o and express this logarithmically, we can transform eq 26 to eq 27 where (logs of) binding constants for reactant and products are replaced by the corresponding pK_a values.

$$\log k_H/k_o = (pK_a^R + pK_a^P)/2 \qquad (27)$$

Sometimes it is possible to compare catalysis by different catalysts, such as protons and metal ions, when it is not possible to measure a rate constant k_o for the uncatalyzed reaction. The ratio of rate constants for the two catalyzed reactions (e.g., k_H/k_M) may then be expressed in terms of differences in binding constants ΔpK_a ($= \log K_B^H - \log K_B^M$) for the protons and metal ions complexed to reactants and products as shown in eq 28.

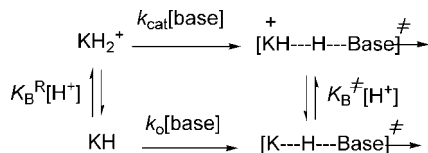$$\log(k_H/k_M) = (\Delta pK_a^R + \Delta pK_a^P)/2 \qquad (28)$$

Phenylacetylpyrazine and Phenacylpyridine. Returning to the comparison of phenylacetylpyrazine and phenacylpyridine,[6] we can now determine how well the differences in catalytic effectiveness of protons and metal ions are represented by their binding constants. Table 6 lists equilibrium constants (shown as pK_a values) for binding protons and zinc ions to the reactants and products of proton transfer from the methylene carbon atoms of the two substrates, with a water molecule acting as a base.

CHART 1

k_H/k_{Zn}	1.54×10^{-3}	2.5	133	1590
pK_a (of enaminone or zwitterion)	2.8	7.4	7.5	12.2

SCHEME 9

From these binding constants values of k_{Zn}/k_H are calculated from eq 28 and compared with experiment for both substrates in Table 6.

In practice, as seen in the right-hand two columns of Table 6, the calculated values of k_{Zn}/k_H for both heterocyclic ketones agree well with experiment. Likewise they account for the great part of the variation between the ketones (1.5×10^6 compared with 6.3×10^6). The values do not depend on assignment of $\alpha = 0.5$ in eq 28 because ΔpK_a^R and ΔpK_a^P are nearly equal (Table 6) and the calculated values of k_{Zn}/k_H are quite insensitive to α.

We may conclude that the greater susceptibility of phenacylpyridine than phenylacetylpyrazine to acid catalysis stems from the stronger binding of the proton to the pyridine than pyrazine ring in both reactants ($pK_a = 5.03$ compared with -1.40) and products ($pK_a = 12.22$ compared with 2.80) and that the difference in the products is augmented by stronger binding of the proton in the resonance-stabilized enaminone than zwitterion (or enol). For zinc ions the difference in Lewis basicity between the two rings is moderated and there seems to be no advantage (over and above that of basicity) of binding the metal to an enaminone than a zwitterion. No doubt this reflects the ability of zinc to coordinate both oxygen and nitrogen basic sites of the zwitterions, whereas the proton is constrained to the latter.

In principle, these conclusions are endorsed by extending comparisons of k_H/k_{Zn} to 2-phenylacetylpyridine and phenacylpyrazine (**5**),[6] which show values intermediate between those for phenylacetylpyrazine and phenacylpyridine (Chart 1). However, while the agreement between calculated and observed values is good for phenylacetylpyridine ($k_H/k_{Zn} = 8.2$ compared with 2.5 observed) the same is not true of phenacylpyrazine, for which 2.5 is calculated but 133 is observed. In the latter case it is possible that other factors, such as a difference in intrinsic barriers for protonation of zwitterions and enaminones,[28] or the hard or soft character of keto binding sites,[18] affect relative magnitudes. However, it is also true that the metal binding constant for phenacylpyrazine (keto tautomer) had to be estimated,[6] and it is possible that this is in error. It seems reasonable to conclude therefore that thermodynamic driving force, as expressed in the binding constants for protons and metal ions in reactants and products, is the dominant influence on the rates of these reactions.

Binding of Catalysts to Transition States. As mentioned above, rate constant ratios comparable to k_H/k_o and k_M/k_o have been characterized as equilibrium constants for "binding catalysts to their

transitions states".[6,33−38] This arises from writing a "kinetic-equilibrium box" in analogy with the thermodynamic box of Scheme 8 (Scheme 9). If the rate constants k_{cat} and k_o are expressed in terms of the pseudoequilibrium constants $K^{\ddagger}$ for formation of their respective transition states, based on the relationship $k = (k_B T/h)K^{\ddagger}$, then a binding constant for the transition state $K_B^{\ddagger}$ may be identified with k_H/k_o through eqs 29 and 30.

$$K_B^{\ddagger}/K_B^R = k_{cat}/k_o \tag{29}$$

$$K_B^{\ddagger} = k_{cat}K_B^R/k_o = k_H/k_o \tag{30}$$

It is clear that $K_B^{\ddagger}$ provides an economical characterization of catalysis. However, to interpret this catalysis normally it must be related to binding of the catalyst to the reactant and product of the catalyzed step, e.g. through the Bronsted relationship of eq 31. In this relationship the binding constant K_B^P usually refers to a reactive intermediate: in the case of phenylacetylpyrazine for example it is an enolate anion. Effective catalysis is then a result of strong binding of the catalyst to a reactant and a reactive intermediate.

$$K_B^{\ddagger} = (K_B^R)^{1-\alpha}(K_B^P)^{\alpha} \tag{31}$$

A further implication of eq 31, already discussed, is that the binding formalism it represents is equivalent to the "conventional" treatment of catalysis in terms of rate and equilibrium constants, based on the identity $k_H/k_o = k_{cat}K_B^R/k_o$ and the more usual form of the Bronsted relationship $k_{cat}/k_o = (K_{cat}K_o)^{\alpha}$. However, as discussed elsewhere,[6] there may be differences of focus, e.g., on the substrate in the binding analysis and on acid or base catalysts in a Bronsted−Marcus treatment.

The tautomerization of heterocyclic ketones lends itself to application of a binding analysis partly because metal−substrate interactions are naturally expressed in terms of binding constants but also because the binding constants to the reactant and product of the rate-determining step are accessible experimentally. In cases where these constants are not readily accessible, the catalysis may still be interpreted qualitatively if the structures of the reactant and product (reactive intermediate) are known or can be inferred. However, for more complex catalysts, including enzymes, the situation may be less straightforward. One complication, which can then arise, is that a conformation change or other equilibrium intervenes between the binding equilibrium of the catalyst and the rate-determining step of the reaction. Alternatively, a covalent reaction may take place between the substrate and the catalyst,[41] or indeed, it may be difficult to identify an uncatalyzed reaction.[6,37] In these cases, the near-to-ideal behavior of the enolization of phenylacetylpyrazine provides a useful comparison for assessing the applicability of (or need to modify) a transition-state-binding treatment.

Conclusions

Keto−enol tautomerism is the dominant tautomerism of phenylacetylpyrazine, in contrast to phenacylpyridine for which an enaminone is the preferred minor tautomer. This reflects a lack of conjugation between the keto group and ring nitrogen atoms of the phenylacetylpyrazine as well as the low basicity of the nitrogens. This low basisicty is also responsible for the

(41) Lienhard, G. E. *Science* **1973**, *180*, 149−154. Bruice, T. C. *Acc. Chem. Res.* **2002**, *35*, 139−148. Braaun-Sand, S.; Olsson, M. H. M.; Warshel, A. *Adv. Phys. Org. Chem.* **2005**, *40*, 201−245.

weak acid catalysis of tautomerization and correspondingly large advantage of metal ions over protons as catalysts. The comparison of proton and metal ion catalysis of enolization (strictly formation of the enolate anion) provides an "ideal" example for analysis in terms of binding of the catalysts to reactants, products, and transition states of a reaction. The close relationship of this analysis to that based on rate−equilibrium relationships and the kinetic effect of thermodynamic driving force is emphasised.

Experimental Section

Synthesis and Materials. A sample of 9-phenylacetylpyrazine was prepared from pyrazine carboxylic acid using a modification of the method employed by Bunting and Stefanidis for the corresponding phenylacetylpyridine.[7] The carboxylic acid was converted to its methyl ester by Fischer esterification and condensed with ethyl phenylacetate to give the α-carbethoxy ester of phenylacetylpyrazine (**15**) as shown in eq 29. The ester was then hydrolyzed and decarboxylated to phenylacetyl pyrazine.
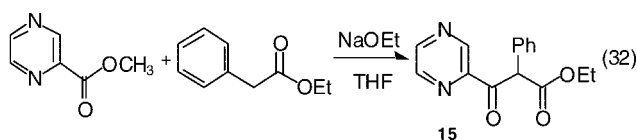
2-Phenyl-2-carbethoxy-1-pyrazinylethanone 15. Phenylethylacetate (5.49 g, 0.033 mol) and methyl pyrazinoate (4.0 g 0.027 mol) in dry THF (30 mL) were added dropwise with stirring to a freshly prepared solution of sodium ethoxide (0.75 g sodium, 0.033 mol) in 12 mL of ethanol. The solution turned orange and then dark red during the course of the addition. It was heated to reflux for 3 h and after cooling poured into water (200 mL). Unreacted starting material was extracted with chloroform and the solution acidified with concentrated sulfuric acid to give a brown semisolid which was extracted with chloroform (3 × 100 mL). The product was dried (Na_2SO_4) and evaporated to give a brown oil which solidified on standing (4.05 g, 60%). A portion of the product (2.5 g) was purified by flash chromatography on silica. Elution with 10:2 hexane/ethyl acetate gave 1.1 g of white solid. ^{1}H NMR (270 MHz, $CDCl_3$) δ: 9.24 (d, 1H, $J = 1.5$ Hz), 8.76 (d, 1H, $J = 2.4$ Hz), 8.68 (dd, 1H, $J = 1.4, 2.4$ Hz), 7.26−7.45 (m, 5H), 6.06 (s, 1H), 4.13 −4.29 (m, 2H, $J = 7.15$ Hz), 1.21 (3H, t, $J = 7.15$ Hz).

2-Phenyl-1-pyrazinylethanone (phenylacetylpyrazine). 2-Phenyl-2-carbethoxy-1-pyrazinylethanone (1.0 g) in 60% aqueous ethanol (100 mL) containing concentrated HCl (1.5 mL) was heated under reflux at 100 °C overnight. Completion of the reaction was checked by TLC after a "mini-workup". Saturated aqueous sodium bicarbonate was added to the reaction mixture which was then extracted with dichloromethane (3 × 100 mL), washed with brine, dried (Na_2SO_4), and evaporated to give a brown oil which solidified on cooling (∼700 mg). The product was purified by flash chromatography on silica using 90:10 hexane/ethyl acetate to give white crystals (∼500 mg). Anal. Calcd for $C_{12}H_{10}N_2O$: C, 72.72; H, 5.09; N, 14.15. Found: 72.16; H, 5.08; N 14.15. ^{1}H NMR (270 MHz, $CDCl_3$) δ: 9.3 (m, 1 H), 8.8 (m, 1H), 8.7 (m, 1H,), 7.2 − 7.5 (m, 5H), 4.5 (s, 2H). ^{13}C NMR (68 MHz, $CDCl_3$) δ: 198.5, 147.8, 147.3, 144.2, 143.5, 133.8, 129.9, 129.9, 128.6, 127.0, 44.2. MS *m/z*: 198 (M^+, 54), 169 (31), 107 (36), 91(100), 65 (40), 52 (32), 39 (18).

Other organic materials were used without purification, including 2-pyrazinecarboxylic acid and 2-acetylpyrazine. Inorganic reagents used for kinetic or equilibrium measurements were generally AR grade (NaCl, NaBr, KI, nickel(II) chloride hexahydrate, and copper(II) nitrate trihydrate). Iodine was GPR grade (resublimed), and bromine was Aristar grade. Zinc(II) nitrate tetrahydrate was a "proanalysi" reagent and Cobalt(II) nitrate trihydrate was a "reinst"

reagent. Anhydrous cadmium chloride was a GPR reagent, as was copper(II) chloride dihydrate

Equilibrium Measurements. Equilibrium and kinetic measurements were performed at 25 °C in aqueous solution. Ionic strengths were usually 0.1 M unless indicated otherwise. Measurements of pK_a values were based on spectrophotometric measurements, described in the Supporting Information, or proton NMR.

The NMR measurements of the protonation of phenylacetylpyrazine and acetylpyrazine were made in solutions of DCl in D_2O in the concentration range $0 - 4.2$ M, and pK_a values in D_2O were obtained from extrapolations based on eq 33 in which X is Cox and Yates's free energy/acidity parameter for correlating medium effects on acid−base equilibria in $DCl-D_2O$,[20] m^* is the slope of the plot of pK_a against X, $K_a = [B][D^+]/[BD^+]$ at the indicated acid concentration and $pK_a(D_2O)$ is the intercept at $X = 0$ (for pure D_2O).

$$pK_a = pK_a(D_2O) + m^*X \qquad (33)$$

Values of K_a were evaluated from eq 34 below in which $δ$ is the chemical shift of the 5-hydrogen atom of the acylpyrazine at the indicated concentration of D_3O^+, and $δ_P$ and $δ_D$ are the limiting chemical shifts at high and low acid concentrations for the protonated and unprotonated heterocycles. Chemical shifts are listed in Tables S1and S2 (Supporting Information), and the data are plotted as $δ$ against $pH − X_o$ in Figures 1 and S1 (Supporting Information). The line through the points in Figure 1 represents a best fit of calculated to experimental chemical shifts for optimized values of $δ_D$, $δ_P$, m^*, and pK_a.

$$K_a = [D^+](δ−δ_D)/(δ_P−δ) \qquad (34)$$

For phenylacetylpyrazine, $pK_a = −0.42 \pm 0.07$ and $m^* = 1.0 \pm 0.25$ and for acetylpyrazine $pK_a = −0.57 \pm 0.07$ and $m^* = 1.4 \pm 0.25$. The large uncertainty in the m^* values reflects the low acid concentrations studied and thus small deviation of pK_a values from those in water.

Kinetic Measurements. Kinetic measurements were carried out using UV−vis spectra to monitor reactions. Directly measured rate constants are generally subject to random errors of ±5%. However, values dissected from combinations with equilibrium constants, from pH profiles or kinetic saturation plots, may be subject to a greater uncertainty, usually noted in the text, and were used to construct the log k_{obs} − pH profiles in Figures 2 and 3 from the inflections of which pK_a values for mono- and di-protonation of the enol were inferred.

First-order rate constants for ketonization of the enol tautomer of phenylacetylpyrazine, k_{obs}, were measured in $HClO_4$, HCl and DCl as described in the Results and Supporting Information. The values are listed in Tables S6 and S9 (Supporting Information) and are plotted as log k against pH or $pH − X_o$ in Figures 2 and 3. The plot against $pH − X_o$ (i.e., for $X_o \neq 0$) refers to concentrated solutions of the acids and is based on modification of eq 9 so that $k_{AH}^{H3O^+}$, K_a^{EH2+} and K_a^{EH3++} are multiplied by the term 10^{m^*Xo}, where m^* is the slope of a plot of log k or pK_a against X_o.[22] As noted above, spectrophotometric evaluation of m^* for the equilibrium constants gives values close to 1.0. Likewise, the near independence of acid concentration of the value of log k_{obs} at high acid concentrations (Figure 2, $pH − X_o < −2$) implies that m_3^* for k_{AH} is close to 1.0. The lines drawn through the data points in Figures 2 and 3 are calculated on this basis and correspond to replacing $[H^+]$ in eq 9 by $10^{(pH−Xo)}$.

It is noteworthy that the pK_a values derived from Figures 2 and 3 have lower values than those determined spectrophotometrically from intial absorbances of the enol or protonated enol from quenching the enolate anion in acid media. For pK_a^{EH2+} and pK_a^{EH3++} in $HClO_4$ the spectrophotometric values are, respectively, 0.45 (0.42 in HCl) and −4.8 compared with kinetic values of −0.58 (−0.41 in HCl) and −7.9. The discrepancy for pK_a^{EH3+2} reflects

the failure of the rate constants in Figure 2 to show a distinct downturn at very negative pH − X_o values and might be dismissed as an unexplained feature of strong acid solutions such as that leading to an *increase* in rate at very negative pH − X_o values in HCl. Similar differences in values for ionization of the enol to its anion, i.e. 9.0 from combining pK_E (2.9) with the spectrophotometrically determined value for ionization of the keto tautomer ($pK_a^{KH} = 11.9$) and 7.7 from the pH profile, may reflect uncertainty in kinetic measurements in borate buffers. However, the values for pK_a^{EH2+} show a consistent discrepancy of one unit both in $HClO_4$ and HCl. It is difficult to find an explanation for this behavior other perhaps than that *E* to *Z* isomerization of an initially formed enol configuration from quenching the enolate anion occurs in competition with reaction of the enol to form its keto tautomer. Such *E* to *Z* isomerization has been observed for enaminone tautomers of other heterocylic ketones.[42] Differences in pK_a values and reactivities of *E* and *Z* enols of α-phenylacetophenone have been reported by Kresge.[43]

Measurements of rate constants for enolization were based on trapping the enol with iodine or bromine in the presence excess iodide or bromide ions as described previously for other heterocyclic ketones.[3] Iodinations were conducted under zero order conditions with a large excess of substrate over the iodine. The standard expression for the rate constant k^E based on measurement of the slope of the linear dependence of absorbance of I_3^- upon time (dA/dt) is given by eq 35, in which [PPz] is the concentration of the phenylacetylpyrazine, $\varepsilon = 2.6 \times 10^4$ is the extinction coefficient of I_3^- and $K_I = 713$ is the association constant between I_2 and I^-. Inclusion of the term $(1 + K_I[I^-])/K_I$ corrects for dissociation of a fraction of the triiodide ion into iodine and iodide ions.

$$k^E = \frac{\Delta A(1 + K_I[I])}{\varepsilon \Delta t[PPZ]K_I[I]} \quad (35)$$

Reversibility of iodination reactions was observed at higher concentrations of hydrogen and iodide ions under the influence of the equilibrium shown in eq 36 and leads to mixed zero- and first-order kinetics. Measurements in 0.008 and 0.018 M $HClO_4$ with 2.0×10^{-3} M phenylacetylpyrazine and 0.02 M KI showed some curvature of plots of absorbance against time but allowed rate constants $k^E = 1.26$ and 1.29×10^{-5} s^{-1} to be determined from measurements of initial slopes.

$$I_3^- + P_Z\text{–H} \rightleftharpoons P_Z\text{–I} + H^+ + 2I^- \quad (36)$$
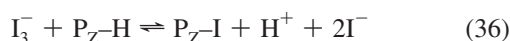
Bromination is less susceptible to reversibility than iodination. Moreover, because of the high rate of reaction and relatively low extinction coefficient of Br_3^- it was possible to work under first order conditions, with a small excess of bromine over substrate (e.g., 4×10^{-3} compared with 2×10^{-3} M), thus avoiding a need to know the concentration of halogen as required of zero order kinetics (eq 32). As shown in Table S12 (Supporting Information),

the measured rate constants in dilute $HClO_4$ show a mild increase with acid concentration. The increase is too large to be attributed to enolization and, as discussed above, may be a result of acid-catalyzed bromination of the pyrazine ring. However, extrapolation to zero acid concentration gave a rate constant $k^E = 1.37 \times 10^{-5}$ s^{-1} in satisfactory agreement with the iodination measurements. A single measurement in DCl and D_2O at an acid concentration too low to affect the rate (0.005M) gave $k^E (D_2O) = 0.57 \times 10^{-5}$ corresponding to an approximate solvent isotope effect $k^E (H_2O)/k^E (D_2O) = 2.4$.

Rate constants for iodination were also measured in 4:1 acetic acid buffers ([AcO$^-$]/ [AcOH]). At the prevailing pH there was no problem with reversibility and the kinetics were consistently zero order. The derived first order rate constants were listed in Table S11 (Supporting Information) and when plotted against concentration of acetate ion gave a second order rate constant for catalysis of enolization by acetate ion of $k_{GB}^E = 2.33 \times 10^{-3}$ M^{-1} s^{-1}.

Rate constants for zinc-catalyzed iodination in the absence of added acid or buffer are recorded in Table S15 (Supporting Information) and show a linear dependence on concentration of zinc ions corresponding to a rate constant $k_{Zn}^E(H_2O) = 3.68 \times 10^{-3}$ M^{-1} s^{-1}. However, as described in the Results, a similar plot for the Zn^{2+} and cacodylate buffer-base catalyzed reaction in 60% TFE−H_2O mixtures ([base] = 8×10^{-4} M, [I$^-$] = 0.005 M) showed distinct curvature with increasing concentration of zinc ions up to the solubility limit of 0.35 M in the mixed solvent. The measured first-order rate constants are shown in Table S16 (Supporting Information) and plotted against [Zn^{2+}] in Figure S3 (Supporting Information). The cacodylate buffer (with 4:1 ratio of buffer base to buffer acid) was chosen to maintain a high enough pH to prevent reversibility of the iodination (cf. eq 33). Rate constants for the Zn^{2+}-catalyzed iodination of acetylpyridine in 60% TFE−H_2O in the absence of buffer are shown in Table S17 (Supporting Information). Comparison of binding constants for the two substrates allowed extrapolation of a value of $K_B = 6.9$ M^{-1} for phenylacetylpyrazine in aqueous solution as already described.

Supporting Information Available: Analysis of *O*- versus *N*-protonation of phenylacetylpyrazine, experimental details of kinetic and equlibrium measurements, Tables S1−S17 containing additional details of rate and equilibrium data referred to in the text; Figure S1, a plot of chemical shifts of a ring proton against acidity for the protonation of acetylpyrazine, Figure S2, a plot of absorbance against acidity for the second protonation of phenylacetylpyrazine enol, Figure S3, a plot of rate constants for iodination of phenylacetyl pyrazine against concentration of zinc ions, and Figures S4 and S5, NMR spectra of phenylacetylpyrazine and 2-phenyl-2-carbethoxy-1-pyrazinylethanone. This material is available free of charge via the Internet at http://pubs.acs.org.

(42) De Maria, P.; Fontana, A.; Spinelli, D. *J. Chem. Soc., Perkin Trans. 2* **1991**, 1067–1070.

(43) Chiang, Y.; Kresge, A. J.; Walsh, P. A.; Yin, Y. *J. Chem. Soc., Chem. Commun.* **1989**, 869–871.

JO802650S